ASIAN JOURNAL OF PHARMACEUTICAL AND CLINICAL RESEARCH

INNOVARE ACADEMIC SCIENCES
Knowledge to Innovation

Vol 11, Issue 3, 2018

Online - 2455-3891
Print - 0974-2441

Research Article

A COMPARISON BETWEEN BIOSORPTION AND BIOACCUMULATION OF FLUORIDE FROM WASTE WATER

TEJ PRATAP SINGH[1], MAJUMDER CB[1]*

[1]Department of Chemical Engineering, Indian Institute of Technology Roorkee, Roorkee - 247 667, Uttarakhand, India.
Email: cbmajumder@gmail.com

Received: 15 December 2017, Revised and Accepted: 27 November 2017

ABSTRACT

Objective: The comparison between the properties of two removal methods viz. adsorptive removal (biosorption) and simultaneous adsorption and bioaccumulation (SAB) of fluoride from waste water was investigated.

Methods: In the present study, bioaccumulation study was done on Sweet Lemon peel. Acinetobacter baumannii (Mtcc no-11451) is a water living microorganism which survives in waste water. Microorganism (Acinetobacter baumannii (Mtcc no-11451)) immobilized on the surface of Sweet Lemon peel. The size of microorganism is greater than the pore size of adsorbent. Active sites of the adsorbent are blocked due to immobilization of microorganism on the surface of adsorbent. Different optimizing parameters are studied during the experiments like adsorbent dose, pH, initial concentration and contact time for bio bioaccumulation process.

Results: It was observed that adsorption and bioaccumulation process execute simultaneously but mainly bioaccumulation is responsible for removal of fluoride. The removal efficiency of fluoride sees a drastic increase from 59.59 % to 99.49 % in optimum conditions. It is to be noted that simple adsorption process removal efficiency was 95.795 % at optimum time (60 min), pH 4.0 and dose 10 g/l. Adsorption isotherm parameters are well fitted for Freundlich whereas simple adsorption follow Langmuir isotherm model.

Conclusion: The removal of fluoride occurred due to the accumulation by bacteria. Kinetic result revealed that bioaccumulation is a slower process. Bioaccumulation process increase the removal efficiency but it is very time consuming and costly as compare to the simple adsorption process.

Keywords: Fluoride, *Acinetobacter baumannii* (Mtcc No. -11451), Sweet lemon peel, Bioaccumulation.

 DOI: http://dx.doi.org/10.22159/ajpcr.2018.v11i3.16604

INTRODUCTION

Biological processes are common phenomenon in our natural ecosystem. In the environment, organic pollutants are generally degraded by simultaneous adsorption and biodegradation/bioaccumulation (SAB). The wastewater from industries such as glass, electroplating, aluminum, steel, chemical industries, and oil refinery contains high fluoride concentration. In general, concentration of fluoride in industrial wastewater varies from 15 mg/l to 20 mg/l after coagulation process. Fluoride is essential as well as toxic for human health. In drinking, water fluoride concentration should not be <0.5 mg/l and not be exceeding 1.5 mg/l. Thus the ever-increasing demand for water has forced the recovery and reutilization of industrial wastewater [1].

The treatment of wastewater is based on SAB which involve basically two types of mechanism. The first one is common effect of microbial cell and adsorbent [2]. The availability of adsorbent increased the liquid-solid interfacial surface for the adsorption of fluoride. Several physicochemical reactions are also possible due to surface catalysis on the surface of adsorbent [3]. Microbial enzymes *Acinetobacter baumannii* immobilized to the surface of adsorbent bring extracellular biodegradation/bioaccumulation of the adsorbed fluoride. As a result of which when SAB occur, the removal efficiency of fluoride and wastewater quality is considerably increased [4]. The second mechanism is mentioned by many authors [5-7]. They reported an opposite result as earlier was described, which explained that there is a steady decrease in the elimination of pollutants, after several adsorption cycles. This mechanism is described by the saturation of the sweet lemon peel surface. In literature, it was also evident that the extracellular microorganisms reaction was not occur inside the micropores of the adsorbent as the size of the microorganisms was larger than the micropores [6]. As a result of which the treatment of wastewater is considered as a result of the combination of the adsorption and the bioaccumulation without any mutual action. The aims of this study were to compare the adsorption and bioaccumulation of fluoride from wastewater.

EXPERIMENTAL

Materials

The following chemicals were used in this research work-sodium chloride, agar, tryptone, yeast extract, Millipore water, sweet lemon peel adsorbents, and bacteria *(A. baumannii).*

Methods

All the chemicals used in this study were obtained from HiMedia Laboratories Pvt., Ltd. Mumbai, India. Stock solution containing 20 mg/l fluoride was prepared by diluting 1 ml of 2000 mg/l fluoride in 100 ml Millipore water (Q-H2O, Millipore Corp. with resistivity of 18.2 MX-cm). Stock solution of 2000 mg/l is prepared by dissolving 0.442 mg of extra pure sodium fluoride in 100 ml of Millipore water. Microbial culture is obtained from MTCC Centre Chandigarh India.

Acclimatization of bacteria (*A. baumannii*)

Here growth indicates toward an orderly increase in the amount of the cellular constituents. It depends on the Calibre of the cell to create new protoplasm from accessible nutrients in the surroundings. Growth curve of bacteria corresponds to increase in cell mass and ribosome, synthesis of the new cell wall, duplication of chromosomes and plasma membrane, septum formation and division of cell. Bacterial population growth studies require inoculation of viable cell into a sterile broth medium and inoculation of the culture under optimum pH, temperature and shaking speed. Under these conditions, the cell will reproduce rapidly, and dynamics of the microbial growth can be charted by means

of a population growth curve which is plotted between increase in number of cells and time.

Batch experiments

For adsorption studies, the batch experiment was conducted in 250 ml round bottom flask with working volume of sample 100 ml containing 14 g/l of adsorbent dose at 30°C and kept in an incubator Cum Orbital Shaker (Metrex, MO-250, India) at 120 rpm. During the experiment, the samples are collected at definite time intervals and spectrophotometrically analyzed for estimating the remaining fluoride concentration. The effect of various parameters such as pH, initial fluoride concentration, contact time, and adsorbent dose was also determined. For SAB study the batch experiment was performed in a 250 ml round bottom flask containing 100 ml of the sample with a little amount of *A. baumannii* and agitated at a constant speed of 120 rpm. Microbial culture grows in 21 h, and dead phase started after 71 h from the study of growth curve of microbial culture. A preliminary test showed that the equilibrium adsorption and bioaccumulation contact time was obtained after 86 h. At the end of this period, the solution samples were taken at definite time intervals and centrifuged at 9000 rpm for 10 min using Remi Laboratory Centrifuge. The supernatant was analyzed through ultraviolet-spectrophotometer at 510 nm wavelength. The bacteria growth was measured as optical density by spectrophotometer (Lasany International) at 600 nm after 86 h and expressed in terms of biomass concentration (mg dry weight/l) [8].

Spectrophotometric methods

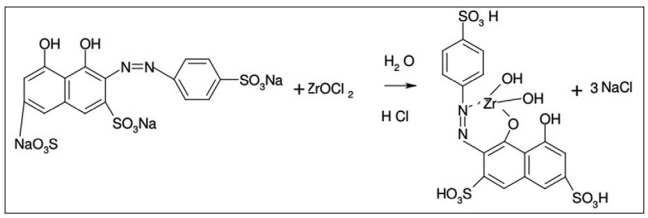

In this technique, a compound of a metal such as aluminum, iron, thorium, zirconium, lanthanum, or cerium reacts with an indicator dye to build a complex of the small dissociation constant. This complex reacts with fluoride to give a new complex. Due to the transformation in the configuration of the complex, the surface assimilation spectrum also shifts relative to the spectrum for the fluoride-free reagent solutions. This alteration can be observed using a spectrophotometer. One of the essential dyes employed is trisodium 2-(para sulfophenyl azo)-1, 8-dihydroxy-3, and 6- naphthalene disulfonate, generally recognized as SPADNS. Eriochrome Cyanine R is one most commonly used dye. The dye reacts with metal ions to give a colored complex. In the SPADNS method, zirconium reacts with SPADNS to build a red colored complex. Fluoride discolors the red color of the complex, and therefore, the alteration in absorbance can be calculated using a spectrophotometer.

Formation of the SPADNS – ZrOCl2 complex

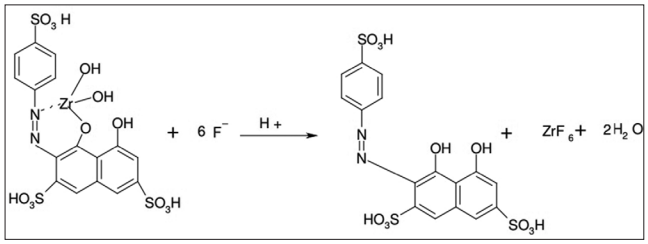

Reaction of the complex with fluoride ions

Recipe for SPADNS solution

$$\frac{\text{Mg of fluoride}}{\text{Litre}} = \frac{A}{\text{Sample(mL)}} \times \frac{B}{C}$$

Where:

1. A represents fluoride obtained by curve (mg).
2. B represents diluted sample final volume (mL).
3. C represents diluted sample volume worn for development of color.

$$\frac{\text{Mg of fluoride}}{\text{Litre}} = \frac{A_0 - A_x}{A_0 - A_1}$$

Where:

1. A_0 represents absorbance at zero fluoride concentration.
2. A_1 represents absorbance at fluoride concentration of 1 mg/L.
3. A_x represents absorbance of sample prepared.

Sterilization

As the bacteria, *A. baumannii* is harmful to human beings and causes infections when disposed into the open environment. Thus, the proper disposal of the bacteria after the bioaccumulation is necessary. For this purpose, we can use the sterilization process that can be achieved through various methods such autoclaves, hot air ovens, sporicidal chemicals, and irradiation. In general, we use the autoclaving method in which the steam is penetrated through the adsorbent for deactivating the bacteria. However, we can also use the irradiation method which is very expensive.

RESULTS AND DISCUSSIONS

pH optimization

Optimization of pH is one of the important parameters. It affects the SAB of the pollutants. From Fig. 1, it was found that for bioaccumulation maximum fluoride removal was 93.14% occurred at pH 4. During SAB, optimum removal of pollutants occurred mostly in pH range of 4–8. From the study it has been observed that there is no significant difference in fluoride removal during pH range of 4–8 as at pH 8, fluoride removal was 92.3%. Thus, we can perform the next optimization parameters such as time, initial concentration, and dose of adsorbents at the neutral pH range so that there is not any effect of acidic or basic medium on bacteria. We are not performing the experiments at pH 4 as water will show acidic nature which results in the deactivation of the bacteria. Similar results were also obtained for biosorption for which maximum fluoride removal is at pH 4, but the further experiments were carried out at pH 7 as for pH range 7–11 the fluoride removal shows a very small difference.

Dose optimization

The effect of adsorbent dose was studied on % fluoride removal by varying the adsorbent dose between 4 and 16 g/l at the 20 mg/l initial fluoride concentration. Microorganism takes the time 21 h to grow, adsorbent is added to immobilize the microorganism at adsorbent surface for 12 h and then pollutant was added. The experiment was carried out at 30°C and 120 rpm for 70 h after the addition of a pollutant. From the nature of the graph as shown in Fig. 2, it seems that

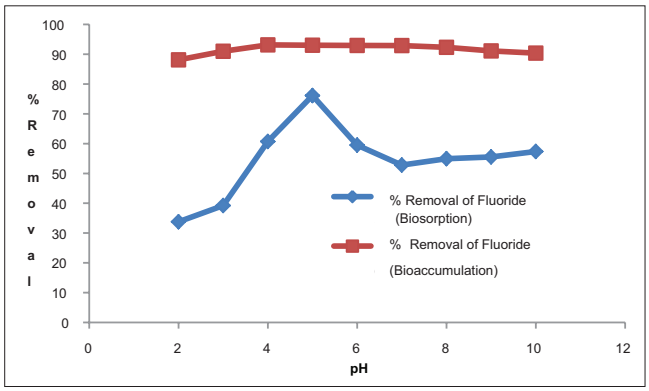

Fig. 1: Graph plotted between the % removal of fluoride and pH

the % removal of fluoride increases up to the 10g/l after which the % removal efficiency is almost same for rest of adsorbent dose. Removal efficiency in between 10 and 16 g/l is almost same (97.95–97.14%) due to this reason the optimum adsorbent dose is 10 g/l. Similarly, for biosorption process, the % removal is almost same ranging from 94.28 to 93.51% for the adsorbent dose of 10–16 g/l. Due to which the optimum adsorbent dose is taken as 10 g/l for other experiments.

Initial concentration

From Fig. 3a, the percentage removal of fluoride decreases when we increase the initial fluoride concentration. In case of bioaccumulation (bioaccumulation) like adsorption, adsorption capacity increases with increase in the concentration of fluoride until the equilibrium was reached for a definite time (87 h). It has been found from the comparison between adsorption and bioaccumulation processes, adsorption capacity, as well as percentage removal for both, is high. Percentage removal of fluoride at equilibrium was obtained 4.47% at 20 mg/l concentration after 87 h.

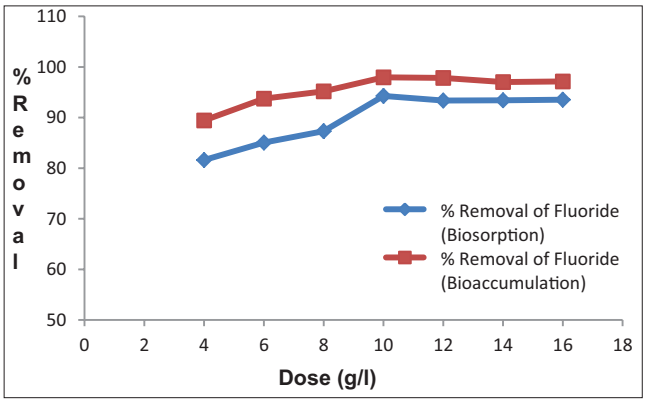

Fig. 2: Graph plotted between the % removal of fluoride and dose and effect of adsorbent dose on the bioaccumulation of fluoride

Contact time

The study of contact time provides the optimum time for the maximum fluoride removal. As shown in Fig. 4a and b the removal of fluoride increases with the increasing contact time for both the processes. The optimum time for the bioaccumulation process is high as compared to the value in case of biosorption for sweet lemon peel adsorbent.

From the comparison Table 1 it was found that the removal of fluoride increased at optimum pH, contact time, dose, and same initial concentration between the biosorption and SAB. The adsorption capacity is also increased for SAB process. For SAB process, the contact time is very high as compare to biosorption.

SAB adsorption kinetics

The governing equation for pseudo-first order model [8,9] is as follows:

$$\log(q_e-q_e)=\log(q_e)-\frac{k_1}{2.303}t \quad (1)$$

Where q_t, q_e (mg/g) are adsorption capacities after time t and at equilibrium correspondingly, and k_1 (h^{-1}) is rate constant for the first-order model.

$$(\frac{mg}{g})/(\frac{mg}{l})^{1/n}$$

Where q_t, q_e (mg/g) are adsorption capacities after time t and at equilibrium correspondingly. K_2 (g mg^{-1} h^{-1}) is rate constant for second-order model.

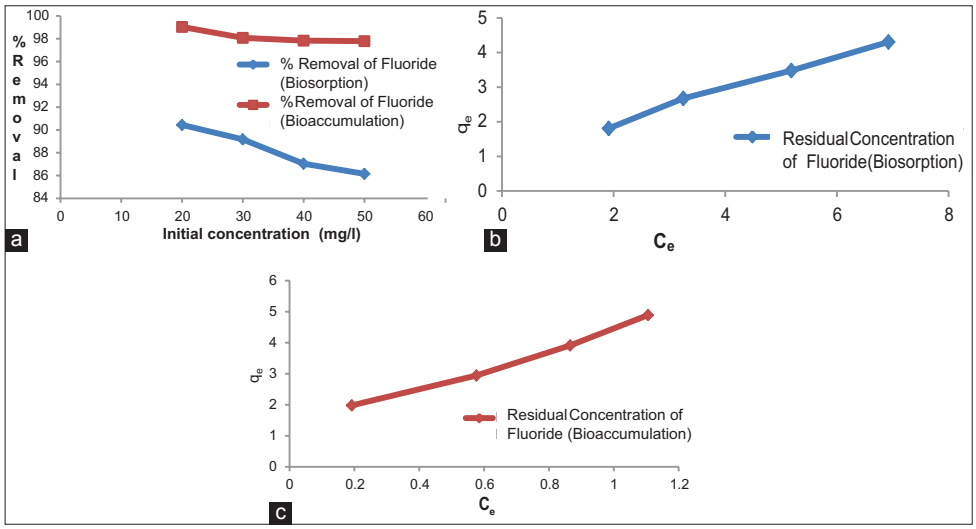

Fig. 3: Graph plotted between (a) % removal and initial concentration (mg/l) (b) residual concentration C_e (mg/l) and adsorption capacity q_e and (c) residual concentration C_e (mg/l) and adsorption capacity q_e (mg/g) for adsorption of fluoride

Table 1: comparative data of optimization parameters between biosorption capacity and bioaccumulation

Process	Initial concentration (mg/l)	Contact Time	Optimum dose (g/l)	Optimum pH	Adsorption capacity q_e (mg/g)	Removal (%)
Biosorption (sweet lemon peel)	20	60 min	10	7	1.91	95.59
SAB (sweet lemon peel)	20	87 h	10	7	1.34	99.49

SAB: Simultaneous adsorption and biodegradation/bioaccumulation

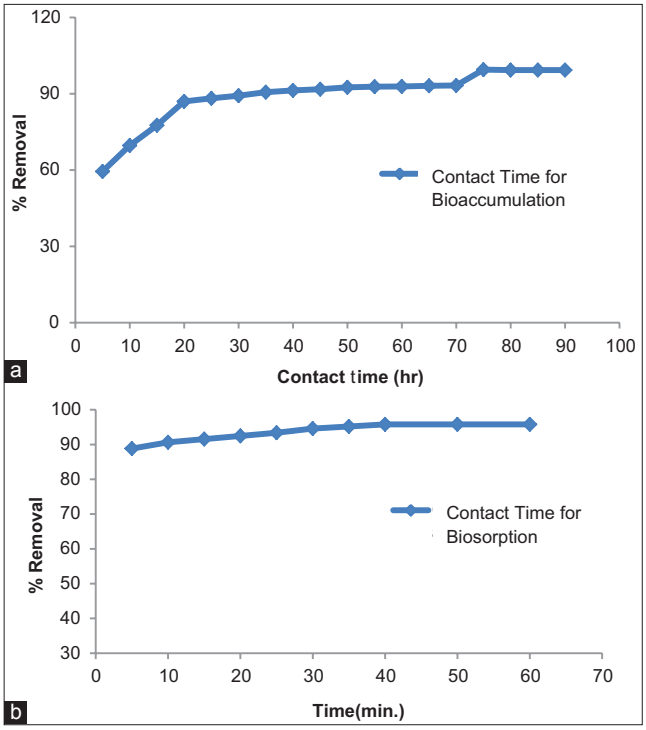

Fig. 4: Graph plotted between (a) % removal of fluoride and contact time (h) on bioaccumulation of fluoride (b) % removal of fluoride and contact time (min) on biosorption of fluoride

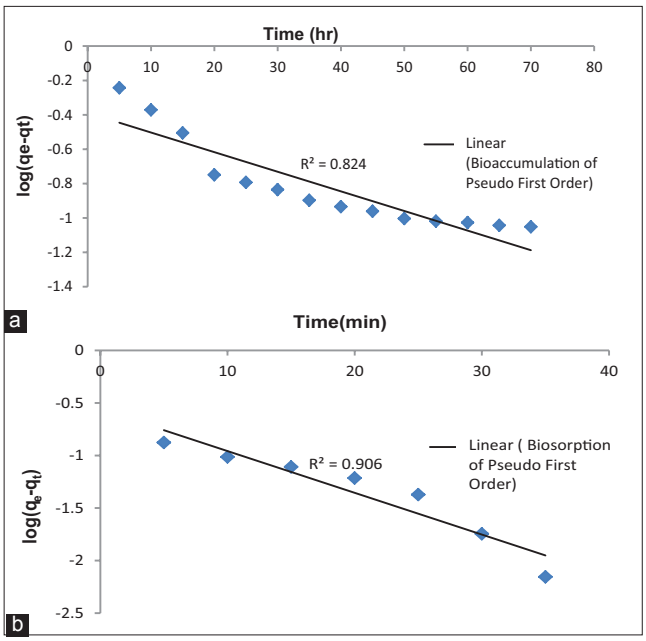

Fig. 5: Pseudo first-order kinetics plotted between (a) log (q_e-q_t) and time (h) for bioaccumulation of fluoride, (b) log (q_e-q_t) and time (min) for biosorption of fluoride The equation for pseudo-second-order model [10] is as follows:

From the comparison Table 2, the adsorption capacity of bioaccumulation process is greater than adsorptive process. In both processes, pseudo-second-order kinetic model is favored due to its greater regression coefficient value. Calculated adsorption capacity q_{ecal} (1.4749 mg/g) for bioaccumulation adsorption is too close to experimental value (q_e=1.421) for second-order kinetics. Similarly, for adsorptive process, experimental value (1.9417 mg/g) is near to the calculated value (1.91 mg/g). Hence, both processes follow the pseudo-second-order kinetic model.

SAB adsorption isotherms

Since SAB and Adsorption are isothermal processes; adsorption isotherms are used to explain these processes. The fundamental importance of the equilibrium adsorption isotherms is the design of adsorption system [8]. Parameters of bioaccumulation equilibrium and adsorption are easily characterized by adsorption isotherms. These parameters are helpful in determining the adsorption capacity of adsorbent materials. To evaluate an adsorption isotherm, it is necessary to develop an equation which precisely represents the results and which may be used for design purpose. Conventional adsorption models are used to describe the equilibrium established between adsorbed component on the adsorbent and unadsorbed component in solution (represented by adsorption isotherms). To analyze the equilibrium data for adsorption and bioaccumulation of fluoride by sweet lemon peel (sweet lemon peel)-immobilized *Acinetobacter*, Langmuir, Freundlich, Temkin, and linear adsorption models were used.

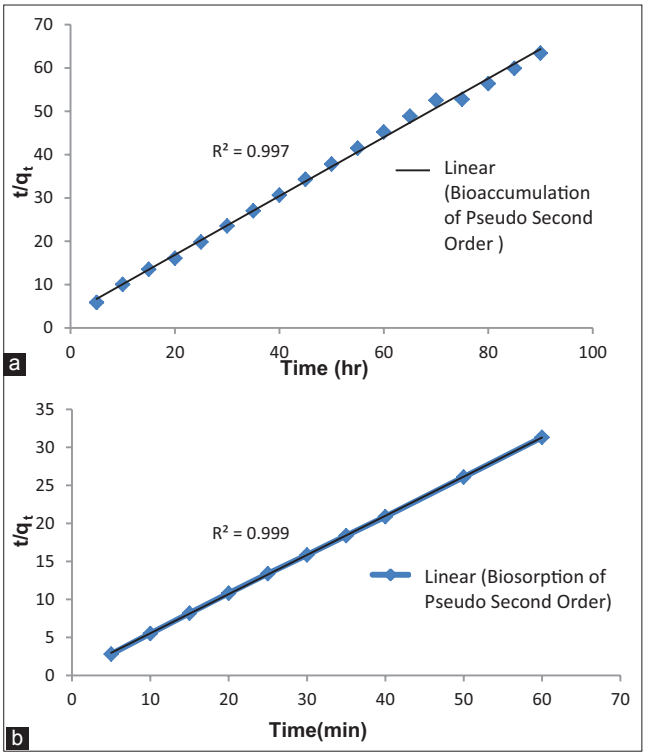

Fig. 6: Pseudo-second order kinetics plotted between (a) t/q_t and time (h) for bioaccumulation of fluoride (b) t/q_t and time (min) for biosorption of fluoride

Table 2: Comparison table for kinetic study in bioaccumulation and adsorption process

Adsorbent	Pseudo-first order			Pseudo-second-order		
	K_1	q_{ecal} (mg/g)	R^2	K^2	q_{ecal} (mg/g)	R^2
SAB (sweet lemon peel)	0.02533(h^{-1})	0.40926	0.824	0.1388 (h^{-1})	1.475	0.997
Adsorption (sweet lemon peel)	0.0898 (min^{-1})	0.2754	0.906	0.686 (min^{-1})	1.942	0.999

Table 3: Comparison of isotherm parameters between adsorptive and bioaccumulation

Process	Adsorbent	Langmuir			Freundlich			Temkin		
		K_l(l/mg)	q_{max} (mg/g)	R^2	K_f $(\frac{mg}{g})/(\frac{mg}{l})^{1/n}$	n	R^2	A_T (l/mg)	b_T (mg/g)	R^2
Adsorption	Sweet lemon peel (sweet lemon peel)	0.1419	8.474	0.9981	1.19	1.511	0.997	1.312	1311.57	0.9861
SAB	*A. baumannii* (sweet lemon peel)	3.202	0.4000	0.9241	0.322	2.14132	0.9521	18.676	222523.38	0.8847

A. baumannii: Acinetobacter baumannii

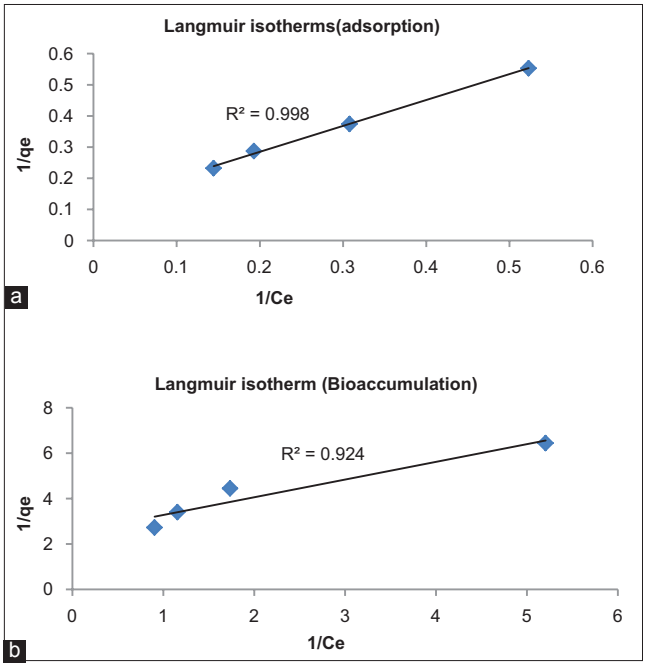

Fig. 7: Graph for Langmuir isotherm model plotted between $1/q_e$ and $1/C_e$ for (a) adsorption isotherm (b) bioaccumulation

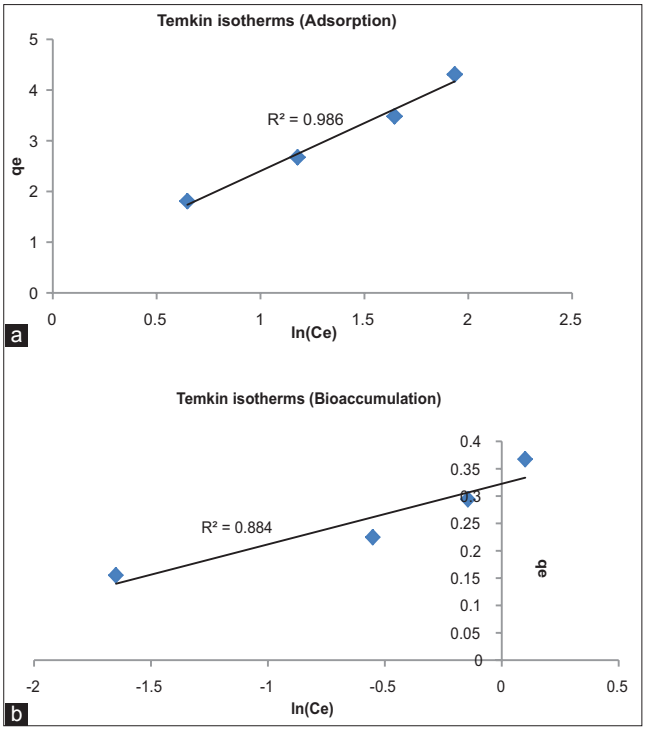

Fig. 9: Graph for Temkin isotherm model plotted between q_e and ln (c_e) for (a) adsorption (b) bioaccumulation

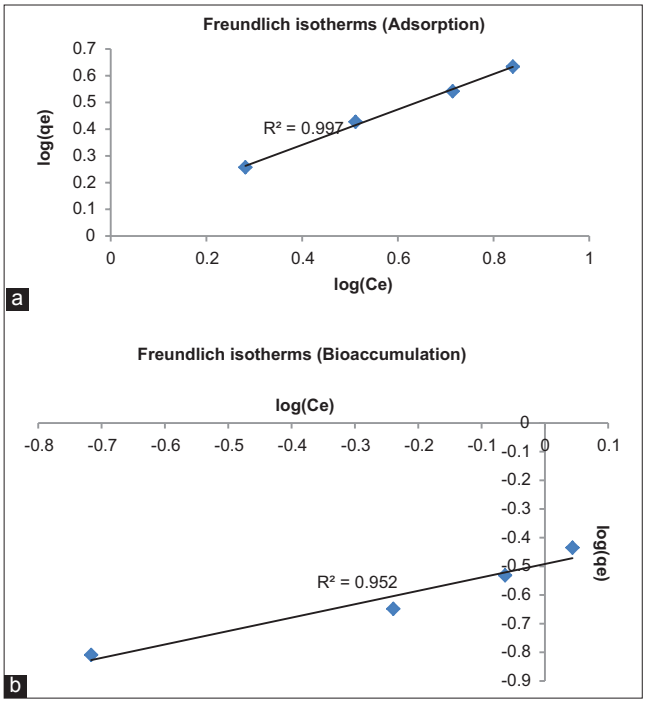

Fig 8: Graph for Freundlich isotherm model plotted between log (q_e) and log (c_e) for (a) adsorption (b) bioaccumulation

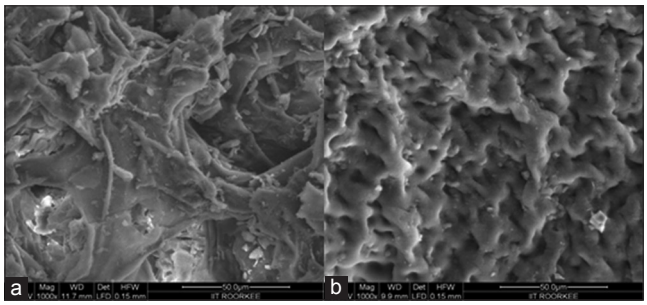

Fig. 10: Scanning electron micrograph of sweet lemon peel (a) before biosorption process (b) after biosorption process

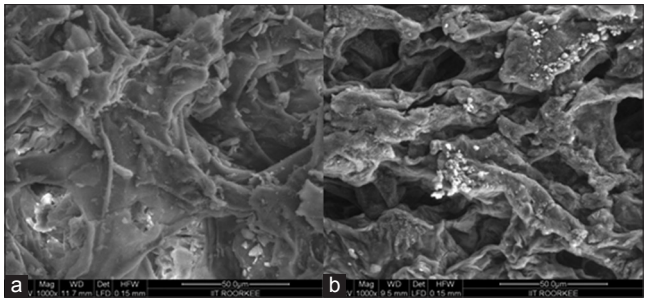

Fig. 11: Scanning electron micrograph of sweet lemon peel (a) before bioaccumulation process (b)

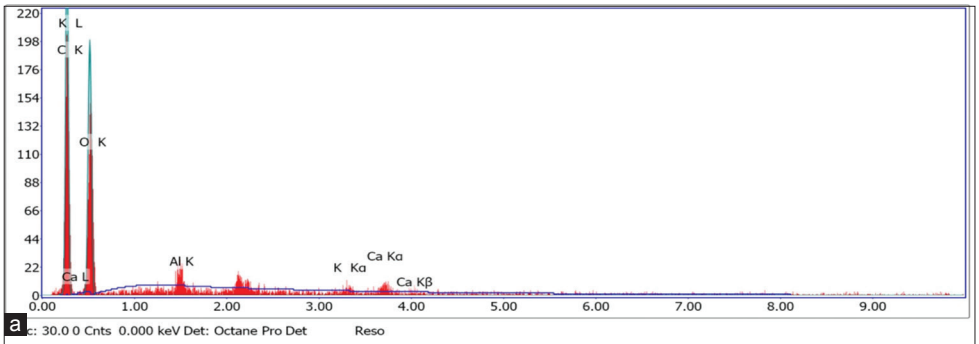

Element	Weight %	Atomic %	Net Int.	Error %
C K	48.97	56.83	65.9	7.16
O K	48.33	42.11	51.49	11.41
AlK	0.61	0.31	2.4	65.56
K K	2.09	0.74	4.99	31.42

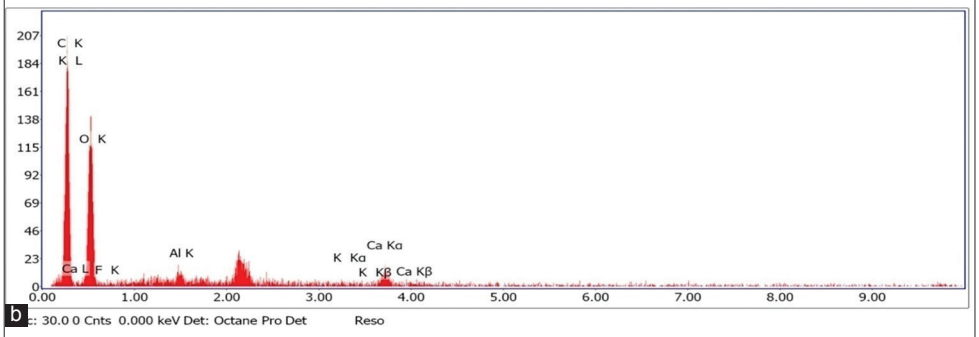

Element	Weight %	Atomic %	Net Int.	Error %
C K	49.57	57.43	60.71	7.57
O K	47.02	40.89	47.97	11.53
F K	0.62	0.45	0.54	86.13
MgK	0.23	0.13	0.78	76.84
AlK	0.63	0.32	2.38	65.93
SiK	0.69	0.34	2.77	63.75
CaK	1.24	0.43	2.34	63.37

Fig. 12: (a) EDAX image of sweet lemon peel before biosorption (b) EDAX image of sweet lemon peel after biosorption

The Langmuir model is as given in equation

$$q_e = \frac{q_m K_l C_e}{1 + K_l C_e} \quad (3)$$

Where K_l and q_m are isotherm constants. Langmuir constant (q_{max}) is fluoride adsorbed per unit weight of adsorbent, at equilibrium time. Langmuir constant (K_l) is energy related to adsorption (i.e., affinity of the binding sites). Langmuir equation is valid for monolayer sorption unto a surface with a finite number of identical sites. The basic assumption of Langmuir model is that sorption takes place at specific sites within the adsorbent. Separation factor is the essential characteristic of Langmuir isotherms which can be described in the equation below:

$$R_L = \frac{1}{1 + K_l C_e} \quad (4)$$

The separation factor (R) indicates the isotherm shape as follows: R<1 unfavorable, R>1 unfavorable, R=1 linear, 0<R<1 favorable, and R=0 irreversible.

The Freundlich isotherm model is given in equation:

$$q_e = K_f C^{1/n} \quad (5)$$

Where, K_f and n are Freundlich constants. K_f is roughly an indicator of the adsorption capacity, and n is the adsorption intensity. The Freundlich isotherm is used for heterogeneous surface energy systems [11]. Temkin Model Equation is given as:

$$q_e = \frac{RT}{b_T} \ln(A_T) + \frac{RT}{b_T} \ln(C_e) \quad (6)$$

Where R is the gas constant, T is temperature (K), q_e adsorption capacity (mg/g), C_e equilibrium concentration (mg/l), and A_T and b_T are the adsorption constants.

From the study of isotherm models for both processes, it has been found that the values of isotherms parameters for all models have increased using bioaccumulation processes as shown in Table 3.

CHARACTERIZATION OF SWEET LEMON PEEL (BIOSORBENT) AND *A. BAUMANNII* MTCC NO.-11451 (MICROBIAL)

Scanning electron micrograph (SEM)

The surface morphology of the sweet lemon peel (sweet lemon peel) examined by SEM Fig. 10a and b through biosorption process and by SEM Fig. 11a and b through the microbial process showing the SEM

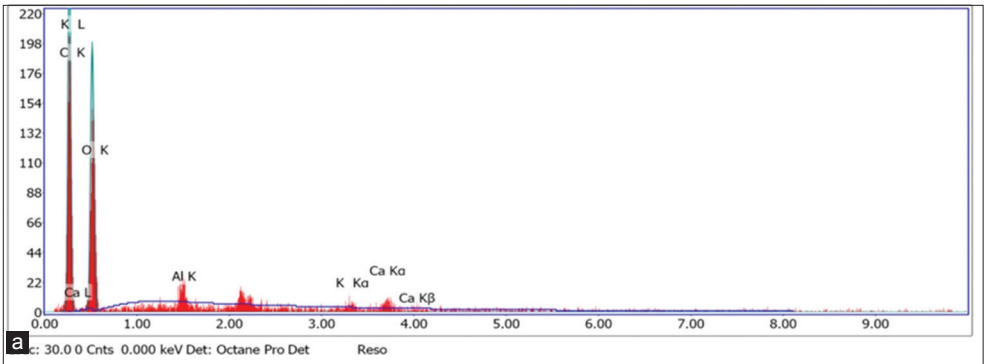

Element	Weight %	Atomic %	Net Int.	Error %
C K	48.97	56.83	65.9	7.16
O K	48.33	42.11	51.49	11.41
AlK	0.61	0.31	2.4	65.56
K K	2.09	0.74	4.99	31.42

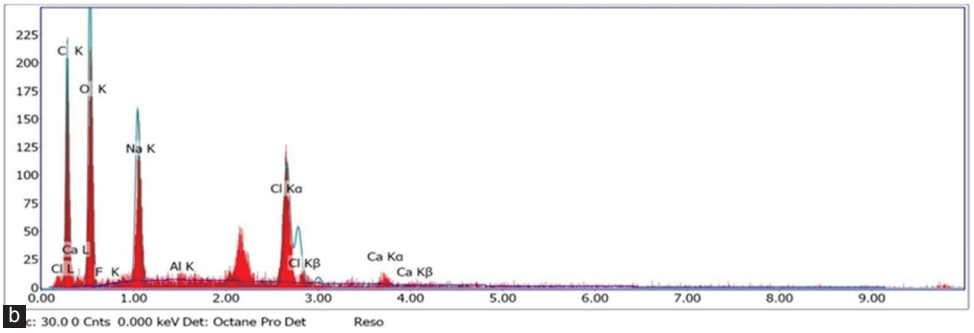

Element	Weight %	Atomic %	Net Int.	Error %
C K	44.1	55.42	61.1	10.98
O K	35.58	33.56	81.1	11.24
F K	0.39	0.31	0.96	81.44
NaK	9.73	6.39	52.92	9.54
AlK	0.22	0.12	1.92	69.1
ClK	8.86	3.77	62.75	6.88
CaK	1.12	0.42	5.05	41.71

Fig. 13: (a) EDAX image of sweet lemon peel before bioaccumulation process (b) EDAX image of sweet lemon peel after bioaccumulation process

Table 4: FTIR analysis for sweet lemon peel using as biosorbent in tabular form

Wave number (cm^{-1})	3400–3500	2500–3300	1550–1650	1370–1390	970–1250
Compound	Amines	Carboxylic acids and derivatives	Amines	Alkanes	Alcohols and phenols
Groups	N-H (1° amines), 2 bands	O-H (very broad)	NH_2 scissoring (1° amines)	CH_2 and CH_3 deformation	C-O

FTIR: Fourier transform infrared spectroscopy

Table 5: FTIR analysis for sweet lemon peel using bioaccumulation process in tabular form

Wave number (cm_{-1})	3400–3500	2500–3300	1550–1650	1370–1390	970–1250
Compound	Amines	Carboxylic acids and derivatives	Amines	Alkanes	Alcohols and phenols
Groups	N-H (1° amines), 2 bands	O-H (very broad)	NH^2 scissoring (1° amines)	CH^2 and CH^3 deformation	C-O

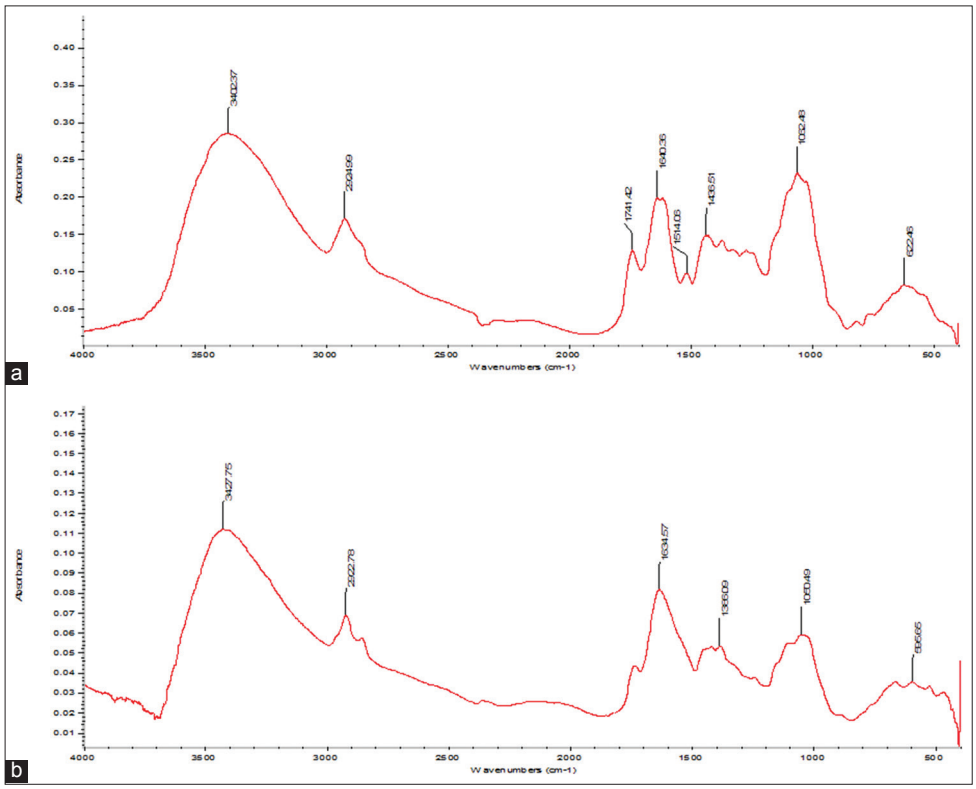

Fig. 14: (a) Fourier transform infrared spectroscopy analysis of sweet lemon peel before biosorption of fluoride (b) Fourier transform infrared spectroscopy analysis of sweet lemon peel after biosorption of fluoride

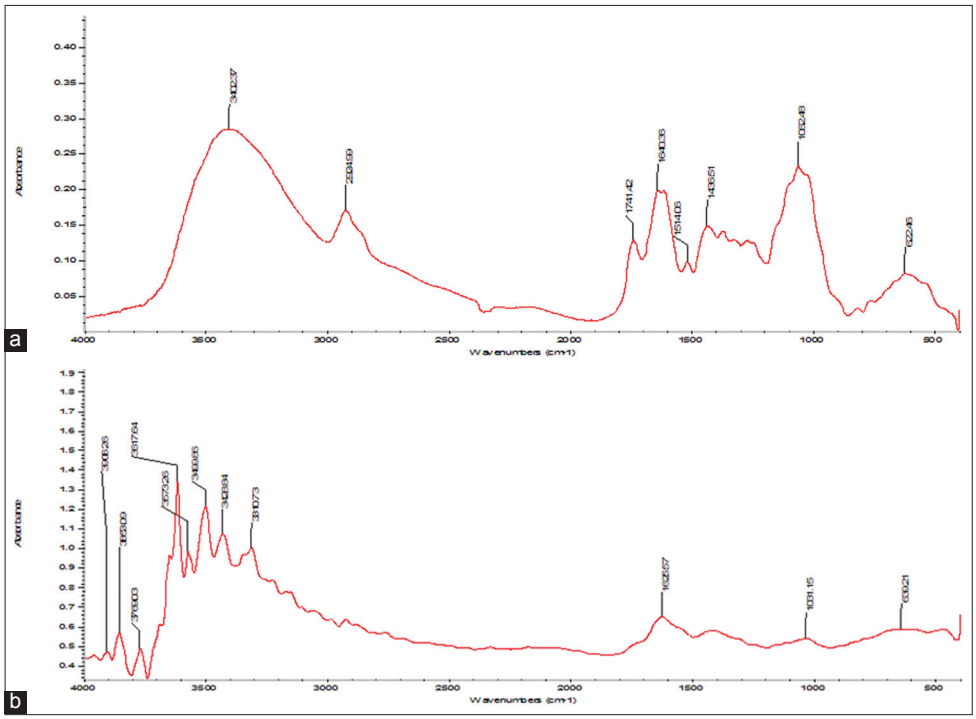

Fig. 15: (a) Fourier transform infrared spectroscopy (FTIR) analysis of sweet lemon peel before bioaccumulation removal of fluoride (b) FTIR Analysis of sweet lemon peel after bioaccumulation removal of fluoride

of sweet lemon adsorbent used for adsorption studies using both biosorption and microbial process. It was revealed from these figs that these adsorbents had irregular and porous surface. The difference in the adsorbent capacity of adsorbent was mainly due to difference in their surface porosity.

EDAX

EDAX of Sweet Lemon before and after biosorption of fluoride ions are shown in Fig. 12a and b and before and after microbial process of fluoride ions removal are shown in Fig. 13a and b. Fig. 12a it is clear that various elements such as carbon, oxygen, and very small amount

of calcium were present in virgin adsorbent but fluoride was not present there. When the EDAX of the biosorbent was carried out after the adsorption of fluorides ion, fluoride was present on the surface of adsorbent about 0.62 wt % which confirmed the adsorption of fluoride by these adsorbents.

Similarly, when the EDAX of the microbial process was carried out after the adsorption of fluorides ion, fluoride was present on the surface of adsorbent about 0.39 wt % which confirmed the adsorption of fluoride by these adsorbent.

Fourier transform infrared spectroscopy (FTIR)

Functional groups present in biosorbents before and after adsorption of biosorbents were determined using FTIR (Thermo Nicolet, Magna 7600). The samples were prepared by pellet (pressed disk) method by mixing the same amount of KBr in each sample. The selected spectral range was from 4000 to 400 cm. Functional groups present on the surface of the peels are determined by the FTIR spectroscopy method. Figs. 14a and b and 15a and b show FTIR spectra on various adsorbents and microbial removal where on the surface of adsorbent and microbes, many functional groups are present (Table 4).

The range of different wave number assign the functional groups present in the adsorbent. The amine bond stretching lies in the wave range of 3400–3500 cm^{-1}, similarly for the very broad O-H (2500–3300 cm^{-1}), NH_2 scissoring stretching (1550–1650 cm^{-1}), alkanes (1370–1390 cm^{-1}), and alcohols and phenols ion stretching (970–1250 cm^{-1}) (Table 5).

CONCLUSIONS

The results obtained from the comparative study show the various differences between biosorption and bioaccumulation such as removal efficiency of bioaccumulation are very high (99.49%) as compared to sweet lemon peel (95.59%). From the adsorption kinetics studies, it is found that the bioaccumulation process is a very slow process as compared to the biosorption process. It follows the pseudo-second order kinetics, and the rate constant for bioaccumulation is less than the biosorption process. It is also found that bioaccumulation process follows the Freundlich isotherm model whereas biosorption process is well suited for Langmuir isotherm model.

REFERENCES

1. Annadurai G, Babu SR, Mahesh KP, Murugesan T. Adsorption and biodegradation of phenol by chitosan-immobilized *Pseudomonas putida* (NICM 2174). Bioprocess Eng 2000;22:493-501.
2. Kalinske AA Enhancement of biological oxidation of organic waste using activated carbon in microbial suspension. Wat Sewage Wks 1972;199:62.
3. Pertotti AE, Rodman CA. Facter involved with biological regeneration of activated carbon. Am Inst Chem Engr Syps Ser 1974;144:316-25.
4. Ehrhardt HM, Rehm HJ. Phenol degradation by micro-organism adsorbed on activated carbon. Appl Microbial Biotech 1985;21:32-5.
5. Craveiro FA, Malina JF Jr. Anaerobic degradation of phenol and bio regeneration of granular activated carbon. J Hazard Wat 1991;28:189-90.
6. Xiaojian Z, Zhangsheng W, Xiasheng G. Simple combination of bio degradation and carbon adsorption -- The mechanism of the biological activated carbon process. Wat Res 1991;25:165-72.
7. Wassenberg DM, Di Giulio RT. Synergistic embryotoxicity of polycyclic aromatic hydrocarbon aryl hydrocarbon receptor agonists with cytochrome P4501A inhibitors in *Fundulus heteroclitus*. Environ Health Perspect 2004;112:1658-64.
8. Afzal M, Iqbal S, Rauf S, Khalid ZM. Characteristics of phenol biodegradation in saline solutions by monocultures of *Pseudomonas aeruginosa* and *Pseudomonas pseudomallei.* J Hazard Mater 2007;149:60-6.
9. Meenakshi S, Viswanathan N. Identification of selective ion-exchange resin for fluoride sorption. J Colloid Interface Sci 2007;308:438-50.
10. Ho YS, Ng JC, McKay G. Kinetics of pollutant sorption by biosorbents: A review. Sep Purif Methods 2000;29:189-23.
11. Lagergran S, Venska KS. About the theory of so-called adsorbtion of soluble substances. Vetenskapsakad Handl 1898;24:1-39.